

Prelude to and Resolution of an Error: EEG Phase Synchrony Reveals Cognitive Control Dynamics during Action Monitoring

James F. Cavanagh,^{1*} Michael X Cohen,^{1,2*} and John J. B. Allen¹

¹Department of Psychology, University of Arizona, Tucson, Arizona 85721, and ²Department of Psychology, The University of Amsterdam, 1018 WB Amsterdam, The Netherlands

Error-related activity in the medial prefrontal cortex (mPFC) is thought to work in conjunction with lateral prefrontal cortex (IPFC) as a part of an action-monitoring network, where errors signal the need for increased cognitive control. The neural mechanism by which this mPFC–IPFC interaction occurs remains unknown. We hypothesized that transient synchronous oscillations in the theta range reflect a mechanism by which these structures interact. To test this hypothesis, we extracted oscillatory phase and power from current–source–density–transformed electroencephalographic data recorded during a Flanker task. Theta power in the mPFC was diminished on the trial preceding an error and increased immediately after an error, consistent with predictions of an action-monitoring system. These power dynamics appeared to take place over a response-related background of oscillatory theta phase coherence. Theta phase synchronization between FCz (mPFC) and F5/6 (IPFC) sites was robustly increased during error trials. The degree of mPFC–IPFC oscillatory synchronization predicted the degree of mPFC power on error trials, and both of these dynamics predicted the degree of posterror reaction time slowing. Oscillatory dynamics in the theta band may in part underlie a mechanism of communication between networks involved in action monitoring and cognitive control.

Key words: theta rhythm; oscillator; cognitive; connectivity; cingulate; human

Introduction

Recent theories of prefrontal cortex functioning postulate that the medial prefrontal cortex (mPFC) interacts with lateral prefrontal cortex (IPFC) in a dynamic loop during goal-directed performance (Botvinick et al., 2001; Ridderinkhof et al., 2004b). This theoretical network uses a monitoring system [putatively mPFC, particularly anterior cingulate cortex (ACC)] to signal the need for enhanced cognitive control (putatively IPFC) during conditions of conflict or after an error. The exact nature of this network remain unexplained, and resolution of this issue has been hindered by the lack of a proposed mechanism for this interaction (Kerns et al., 2004; Ridderinkhof et al., 2004a,b). In this report, evidence is presented that neural oscillatory mechanisms might underlie functional communication between action-monitoring and cognitive control networks across mPFC and IPFC regions.

The integrity of the action-monitoring system appears to decline on trials preceding response errors. Error-preceding trials

are characterized by progressively faster reaction times (Gehring and Fencsik, 2001), decreases in PFC activity, and an increase in default-mode activation (Weissman et al., 2006; Eichele et al., 2008), and alteration of the event-related potential (Ridderinkhof et al., 2003) that may be reflective of a smaller response-locked neuroelectric signature (Allain et al., 2004). Convergent evidence suggests that a transition from a goal-directed state to an inattentive state may hinder performance by contributing to a failure to attend to incoming stimulus-response mappings. After an error, the action-monitoring system (mPFC) is proposed to function as an alarm, recruiting the control network (IPFC) to reallocate attention or increase the motor threshold (Botvinick et al., 2001; Eichele et al., 2008). Posterror reaction time slowing is commonly used as a measurement of instantiated cognitive control, because error-following trials are characterized by a deliberate alteration of the speed/accuracy trade-off. Posterror slowing has been predicted by ACC and IPFC activity after errors (Garavan et al., 2002; Kerns et al., 2004; Kerns, 2006; Hester et al., 2007), but these studies have not revealed how the proposed monitoring and control systems interact.

Synchronized neural oscillations may be one mechanism by which different regions within a network (e.g., mPFC and IPFC) can interact (Engel and Singer, 2001; Fries, 2005). A growing body of work is focusing on the oscillatory characteristics of frontal midline theta (4–8 Hz) in the generation of the EEG signature of errors, the error-related negativity (ERN) (Luu et al., 2004; Trujillo and Allen, 2007). The ERN may provide a sensitive index

Received Aug. 29, 2008; revised Oct. 30, 2008; accepted Nov. 26, 2008.

This work was supported by infrastructure provided by National Institute of Mental Health (NIMH) Grant R01-MH066902. J.F.C. is supported by NIMH Grant F31MH082560. We thank Jürgen Kayser and Craig Tenke for their help with the application of their CSD scripts, and Christina Figueroa for help with data collection.

*J.F.C. and M.X.C. contributed equally to this work.

Correspondence should be addressed to James F. Cavanagh, Department of Psychology, University of Arizona, 1503 University Avenue, Tucson, AZ 85721. E-mail: jimcav@email.arizona.edu.

DOI:10.1523/JNEUROSCI.4137-08.2009

Copyright © 2009 Society for Neuroscience 0270-6474/09/290098-08\$15.00/0

of both decreases (Allain et al., 2004) and error-related increases (Yeung et al., 2004a) of the action-monitoring system. Additionally, the ERN has been shown to correlate with both error-related ACC activation and posterror reaction time slowing (Debener et al. 2005), possibly providing an index of cognitive control. Given the theta oscillatory dynamics of the ERN, oscillatory phase synchrony between mPFC and lPFC in the theta band is a plausible and untested mechanism for the collaborative functioning of action-monitoring and cognitive control networks.

Materials and Methods

Participants. Fourteen introductory psychology students (six female; mean age, 18.86; \pm SD, 0.95) served as participants to partially fulfill a research experience requirement for their class. All participants were free from past neurological trauma, had normal or corrected-to-normal vision, and were free from current psychoactive medication use. The data from these 14 participants were taken from another study (T. O. C. Gründler, J. F. Cavanagh, C. M. Figueroa, M. J. Frank, and J. J. B. Allen, unpublished data) investigating obsessive-compulsive symptomatology. Note that the 14 participants used for the present study had normative levels of obsessive-compulsive symptomatology (obsessive-compulsive inventory-revised scores: mean, 8.6; SD, 6.8; range, 0–17). All participants gave informed consent before participating.

Procedure. Participants completed a modified Eriksen Flankers task (Eriksen and Eriksen, 1974; Eriksen and Schultz, 1979) which has been described in detail in previous reports (Cavanagh and Allen, 2008; Gründler, Cavanagh, Figueroa, Frank, and Allen, unpublished data). On each of the 400 trials in this speeded response task, participants were required to press one of two hand-held response buttons with their thumbs to identify the center letter in a string that is either congruent (i.e., MMMMM or NNNNN; 200 trials total) or incongruent (i.e., NNMNN or MMNMM; 200 trials total) from the flankers. The target–hand mappings were reversed between consecutive blocks to increase response conflict. Errors were likely to occur on incongruent trials, attributable to increased response competition, or after target–hand switches. EEG was recorded from 62 channels on the scalp using a stretch-lycra Ag–AgCl electrode cap. Mastoid sites, vertical and horizontal ocular sites (vertical electro-oculogram and horizontal electro-oculogram) were recorded with drop electrodes. All sites were grounded anterior to Fz and referenced online posterior to Cz. Data were sampled at 500 Hz, amplified 500 \times , with a bandpass of 0.05–100 Hz, and impedances were <10 K Ω .

Task and EEG recording. A matching algorithm was used to match trials for reaction time (RT), selecting the correct trial with RT closest to each erroneous response. Response-locked epochs were obtained for these trials (N), as well as the two trials preceding (N-2 and N-1) and after (N+1 and N+2) each error and matched correct trial. All EEG data were visually inspected for artifacts, and epoched from –1000 to +2000 ms peri-response, with large windows to accommodate edge artifacts induced by wavelet convolution. Eye blinks were corrected using a regression algorithm. All participants had EEG data for at least 29 erroneous responses and at least 20 epochs for single-trial analyses. All EEG epochs were then converted to current source density (CSD) using the methods of Kayser and Tenke (2006). CSD computes the second spatial derivative of voltage between nearby electrode sites, acting as a reference-free spatially enhanced signal representation. The CSD transformation highlights local electrical activities at the expense of diminishing the representation of distal activities (volume conduction). The diminishment of volume conduction effects by CSD transformation may reveal subtle local dynamics and also lead to more accurate characterization of local activities during the calculation of long-distance coherence. All CSD-event-related potentials (ERPs) were created at the FCz electrode by filtering (1–15 Hz), baseline correcting (–100 to 0 ms), and cutting the length (–300 to +500 ms) of each raw CSD epoch before averaging. CSD–ERPs were measured as the size of the difference between the largest trough (between 0 and 120 ms) and the preceding peak, with a larger CSD–ERP component (i.e., a more negative ERN) quantified as a larger positive value.

Time–frequency calculation. Time–frequency calculations were com-

puted using custom-written Matlab (The MathWorks) routines (Cohen et al., 2008). Power and intertrial phase coherence (ITPC) were calculated for the raw CSD–EEG epochs at electrode FCz. The CSD–EEG time series in each epoch was convolved with a set of complex Morlet wavelets, defined as a Gaussian-windowed complex sine wave: $e^{-i2\pi ft} e^{-t2/(2\sigma^2)}$, where t is time, f is frequency (which increased from 2.5 to 50 Hz in 30 logarithmically spaced steps), and σ defines the width (or “cycles”) of each frequency band, set according to $4.5/(2\pi f)$. A width of 4.5 provides an adequate trade-off between temporal and frequency resolution (Trujillo and Allen, 2007). We also reran the analyses using three cycles (greater temporal resolution at the expense of frequency resolution) (supplemental Fig. S1, available at www.jneurosci.org as supplemental material). From the resulting analytic signal, we obtained the following: (1) estimates of instantaneous power (the magnitude of the analytic signal), defined as $Z(t)$ (power time series: $p(t) = \text{real}[z(t)]^2 + \text{imag}[z(t)]^2$); and, (2) phase (the phase angle) defined as $\phi_i = \arctan(\text{imag}[z(t)]/\text{real}[z(t)])$. Each epoch was then cut in length (–300 to +500 ms peri-response) and baseline corrected to the average frequency power from –300 to –100 ms before the onset of the cue (Cohen et al., 2008). Power was normalized by conversion to a decibel (dB) scale ($10 \cdot \log_{10}[\text{power}(t)/\text{power}(\text{baseline})]$), allowing a direct comparison of effects across frequency bands.

Two different types of oscillation phase coherence were examined: intertrial phase coherence and interchannel phase synchrony (ICPS). ITPC measures the consistency of phase values for a given frequency band at each point in time over trials, in one particular electrode. Phase coherence values vary from 0 to 1, where 0 indicates random phases at that time–frequency point across trials, and 1 indicates identical phase values at that time–frequency point across trials. The phase coherence value is defined as follows:

$$\text{ITPC} = \frac{1}{n} \sum_{x=1}^n e^{i\phi_{xi}}$$

where n is the number of trials for each time and each frequency band. ITPC thus reflects the extent to which oscillation phase values are consistent over trials at that point in time–frequency space (power, in contrast, represents the intensity of that signal). Note that this measure of phase coherence does not differentiate between possible biophysical mechanisms underlying phase consistency, such as phase reset or phase “smearing.” Rather, this measure simply indicates the statistical probability of increased phase consistency between trial and baseline epochs. The hypotheses for the current investigation require comparing these measures of phase consistency across conditions, not comparing the difference in underlying biophysical mechanisms, per se.

ICPS measures the extent to which oscillation phases are similar across different electrodes over time–frequency. ICPS is calculated in a similar manner as intertrial phase coherence as follows:

$$\text{ICPS} = \frac{1}{n} \sum_{t=1}^n e^{i[\phi_j - \phi_k]}$$

where n is the number of trials, ϕ_j and ϕ_k are the phase angles of electrode j and k . Thus, phase angles are extracted from two electrodes and then subtracted: if the phase angles from the two electrodes fluctuate in synchrony over a period of time, their difference will be constant (i.e., non-uniformly distributed), leading to ICPS values close to 1. All ICPS values were computed as the percentage change from the precue baseline. For convenience, we use the term “coherence” when describing the consistency of phase angles over trials within a single electrode (ITPC), and the term “synchrony” when describing the consistency of phase angles between two channels (ICPS).

For this investigation, F5–FCz and F6–FCz sites were used to measure phase synchrony between mPFC and lPFC. To rule out an alternative explanation of volume conduction effects, ICPS was also calculated between CP3–FCz and CP4–FCz: these pairs are of similar spatial difference between F5/6 and FCz in the posterior direction (closest Euclidean

distance), but no theories postulate a role for these posterior areas in the type of cognitive control under investigation here. We selected both F5 and F6 phase synchrony because the literature does not provide a clear indication about whether PFC-based cognitive control is lateralized (Garavan et al., 2002; Kerns et al., 2004; Kerns, 2006; Hester et al., 2007). For the trial-averaged analyses, ICPS was calculated for each time point over trials, using the equation above. For the single-trial analyses, ICPS was calculated at each trial over time points. Here, the equation was the same, but n now refers to the number of time points instead of number of trials. Based on the time–frequency analyses shown in Figures 2 and 3 and supplemental Figure S1, available at www.jneurosci.org as supplemental material, two analytic windows around the response were chosen for quantification of theta-band activities (4–8 Hz): (–100 to 300 ms) and (0 to 200 ms).

Statistical analysis. All power, ITPC, and ICPS measures were quantified as the average value and time of peak. For clarity and simplicity, only the error/correct trials (N) and immediately surrounding trials (N–1 and N+1) in the wide (–100 to 300 ms) window were entered into statistical analyses of averaged values. Separate 2 (accuracy: error, correct) \times 3 (trial: N–1, N, N+1) ANOVAs were run for each measure, with an expected accuracy by trial quadratic interaction. For ICPS measures, additional tests were conducted to examine laterality by mirroring the 2 \times 3 ANOVA, but with an additional (hemisphere: right F6, left F5) dimension, with an expected accuracy by trial interaction in the absence of a lateralized effect. The spatial specificity of the ICPS on trial N was tested with a 2 (accuracy: error, correct) \times 2 (hemisphere: right, left) \times 2 (caudality: anterior F5/6, posterior CP3/4) ANOVA, with an expected accuracy by caudality interaction. Where appropriate, follow-up paired-samples t tests (error vs correct) were conducted to test specific a priori hypotheses. Single-trial analyses were performed on error and error-following trials. Individual standardized β weights were taken from bivariate regressions between a priori determined measures of conflict-control activities (ICPS and FCz power) and posterror reaction times (from posterror trials which were answered correctly), within two different analytic windows: (–100 to 300 ms) and (0 to 200 ms).

Results

Behavioral performance

Participants made an average of 60.1 (\pm SD, 52.2) errors on the task, with errors on incongruent trials consisting of 70% of total errors. EEG data were available for an average of 52.2 (\pm SD, 20.1) errors, and all subsequent behavioral analyses were performed on these errors (and RT-matched correct trials). Participants self-corrected on an average of 53% (\pm SD, 29%) of these error trials, although this proportion varied widely across participants. There were similar RTs for error (mean, 427.0; \pm SD, 71.0) and reaction time matched correct trials (mean, 438.7; \pm SD, 63.1). Participants displayed reliable posterror reaction time slowing (mean, 79.4; \pm SD, 22.9; one-sample t test: $t_{(13)} = 12.47$; $p < 0.001$; d , 3.46), shown in Figure 1A.

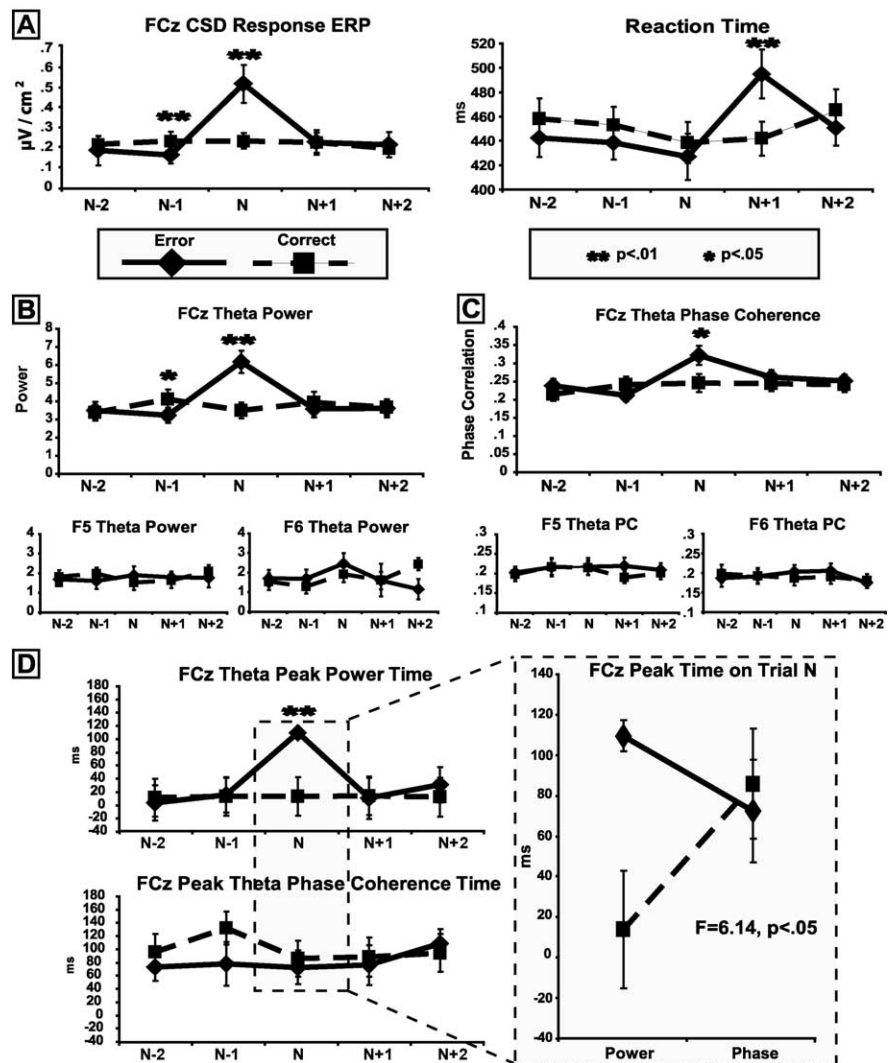


Figure 1. Time courses of CSD activities (mean \pm SE). **A**, CSD–ERPs show decreased activity preceding an error and increased activity immediately after an error. The reaction time plot shows posterror slowing. **B**, Averaged FCz (mPFC) power demonstrates similar dynamics as the CSD–ERP, but F5 and F6 (IPFC) sites show no accuracy difference. **C**, Averaged FCz intertrial phase coherence increases after errors, but F5 and F6 sites show no difference. Note that ordinate scaling on FCz plots in **B** and **C** are 200% of the F5 and F6 ordinate. **D**, Differences in peak latency for power and phase coherence at the FCz site. This accuracy-related difference shows that phase coherence latency is constant, but peak power occurs much later after an error.

ERP analyses

The CSD–ERP 2 \times 3 ANOVA revealed a significant accuracy by trial interaction ($F_{(1,13)} = 17.8$; $p < 0.001$; partial $\eta^2 = 0.58$), and follow-up t tests indicated that the CSD–ERP was larger on error trials ($t_{(13)} = 3.4$; $p < 0.01$; $d = 0.90$) and smaller on error-preceding trials ($t_{(13)} = -2.8$; $p < 0.01$; $d = 0.75$) compared with each corresponding correct trial. These data replicate previous investigations of a diminished response-locked voltage negativity immediately preceding errors (Allain et al., 2004), and a large response-locked voltage negativity (ERN) directly after error commission (Figs. 1A, 2A).

mPFC theta frequency dynamics

The CSD–ERN from the ERP analysis significantly correlated with theta power ($r_{(14)} = 0.57$; $p < 0.05$, $R^2 = 0.32$) and ITPC values ($r_{(14)} = 0.64$; $p < 0.01$; $R^2 = 0.45$), indicating a large degree of shared variance between ERP, power, and phase coherence measures immediately after an error. Figure 2 shows com-

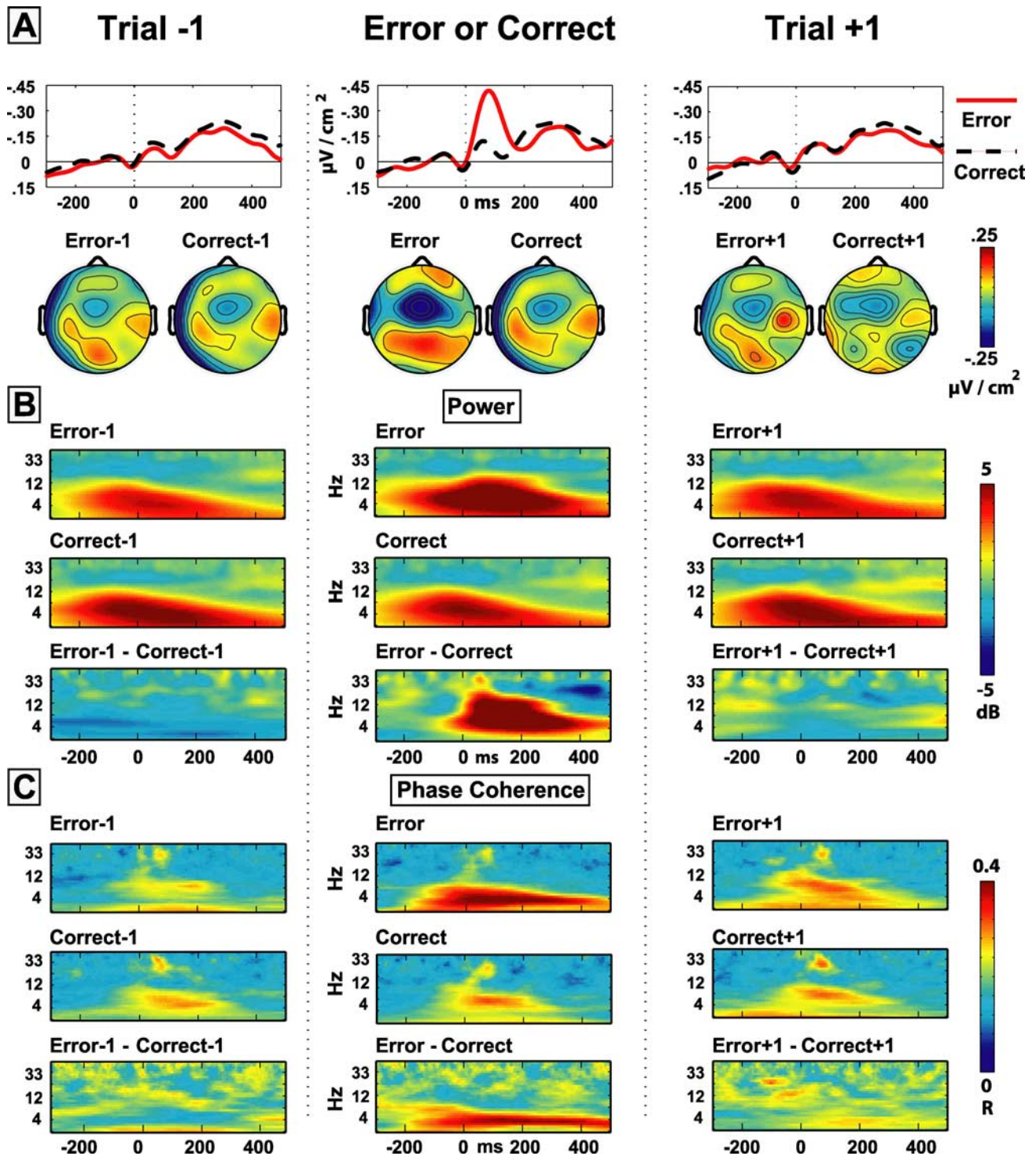


Figure 2. Response locked CSD grand averages for N-1 (left), N (center), and N+1 (right) trials. **A**, CSD-ERPs and topographic maps. Topographic maps reflect the average from 50 to 90 ms after the response. **B**, Power in dB. Note the latency of error trial power compared with all other power plots. The error–correct contrast reveals a large burst of power in the theta and low alpha range after an error. **C**, Intertrial phase coherence (R). Note the increase of phase coherence after an error, especially ~ 4 Hz.

plementary perspectives of ERP, power, and phase coherence measures for error and peri-error trials. Similar to the CSD-ERN findings, the theta power value 2×3 ANOVA revealed a significant accuracy by trial interaction ($F_{(1,13)} = 22.6$; $p < 0.001$; partial $\eta^2 = 0.64$), and follow-up t tests indicated that power was larger on error trials ($t_{(13)} = 4.8$; $p < 0.001$; $d = 1.28$) and smaller on error-preceding trials ($t_{(13)} = -2.4$; $p < 0.05$; $d = 0.65$) compared with each corresponding correct trial (Fig. 1B). The ITPC

value 2×3 ANOVA also revealed a significant accuracy by trial interaction ($F_{(1,13)} = 5.0$; $p < 0.05$; partial $\eta^2 = 0.28$), where ITPC was greater on error trials ($t_{(13)} = 2.6$; $p < 0.05$; $d = 0.68$), but there was no effect for error-preceding trials compared with the corresponding correct trial (Fig. 1C). Similar statistical tests were run for each IPFC site (F5 and F6) separately. There were no significant 2×3 ANOVA interactions or single-trial t tests for F5 or F6 power value or ITPC value (Fig. 1B, C).

mPFC theta frequency dynamics: peak latencies

The peak power latency 2×3 ANOVA revealed a significant accuracy by trial interaction ($F_{(1,13)} = 10.3$; $p < 0.01$; partial $\eta^2 = 0.44$), whereby peak power latency was longer after errors compared with the corresponding correct trial ($t_{(13)} = 3.2$; $p < 0.05$; $d = 0.86$). Peak ITPC latency did not differ between error and correct trials. Complementary statistical tests were run for each IPFC site (F5 and F6) separately. There were no significant 2×3 ANOVA interactions or single-trial t tests for F5 or F6 peak power latency or peak ITPC latency. An additional ANOVA was used to investigate the difference between the longer mPFC peak power latency and constant mPFC peak ITPC latency on error trials. A 2 (accuracy: error, correct) $\times 2$ (measure: peak power time, peak ITPC time) ANOVA revealed a significant interaction ($F_{(1,13)} = 6.1$; $p < 0.05$; partial $\eta^2 = 0.32$), where ITPC remained temporally constant yet power increased ~ 100 ms later after errors compared with the corresponding correct trial measures (Fig. 1D).

Summary of mPFC activities

Error trials may be predicted by a decline in response-related mPFC power on the preceding trial. Error-related mPFC activities consist of an increase in both ITPC and power values. Although ITPC occurs at the same time on error and correct trials, a prolonged peak latency of the power burst appears to be specific to error trials. There were no significant 2×3 ANOVA interactions or single-trial t tests for F5 or F6 power value, peak power time, ITPC value, or peak ITPC time, indicating that these power and ITPC effects are specific to the mPFC and are not seen in IPFC sites.

Theta frequency interchannel phase coherence

The ICPS between mPFC and IPFC was robustly increased on error trials, as demonstrated by the significant accuracy by trial interaction ($F_{(1,13)} = 15.4$; $p < 0.01$; partial $\eta^2 = 0.54$), with no main or interaction effects for hemisphere. Follow-up t tests indicate that both F5–FCz ($t_{(13)} = 2.6$; $p < 0.05$; $d = 0.70$) and F6–FCz ($t_{(13)} = 2.8$; $p < 0.05$; $d = 0.75$) pairs demonstrated significantly greater ICPS on error compared with correct trials. Focusing just on trial N, the increased ICPS with mPFC was specific to these IPFC sites (not CP3/4 sites), as demonstrated by a significant accuracy \times caudality interaction ($F_{(1,13)} = 5.9$; $p < 0.05$; partial $\eta^2 = 0.31$) with no main or interaction effects for hemisphere. These findings indicate that error trials alone are characterized by increased mPFC–IPFC connectivity as measured by ICPS in the theta band, as shown in Figure 3.

Single-trial analysis

Figure 4 displays the results of the single-trial analyses. One sample t tests of the individual standardized β weights revealed that ICPS predicted FCz theta power during errors between both F5–

Inter-Channel Phase Synchrony Change

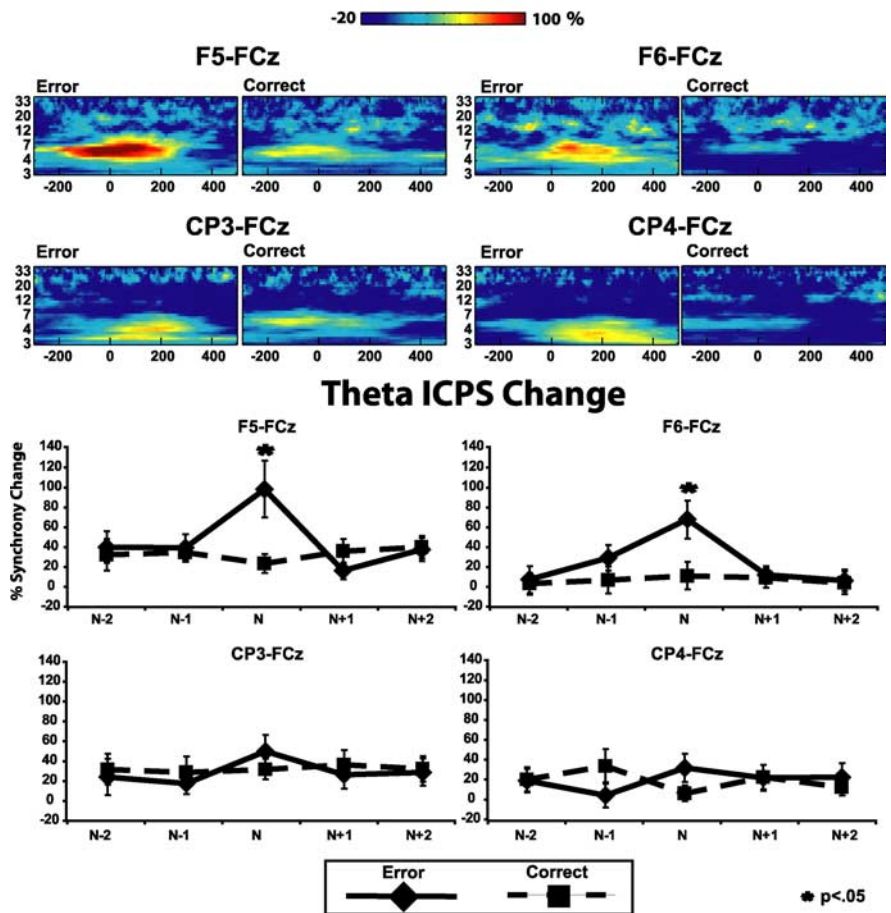


Figure 3. Grand-averaged interchannel phase synchrony calculated as a percentage change from baseline. ICPS is increased after errors, with robust increases in the theta band at frontal sites.

FCz (-100 to 300 ms: $t_{(13)} = 6.71$, $p < 0.001$, $d = 1.79$; 0 to 200 ms: $t_{(13)} = 7.01$, $p < 0.001$, $d = 1.87$) and F6–FCz sites (-100 to 300 ms: $t_{(13)} = 2.42$, $p < 0.05$, $d = 0.64$; 0 to 200 ms: $t_{(13)} = 2.48$, $p < 0.05$, $d = 0.66$). Both peak theta power at FCz (-100 to 300 ms: $t_{(13)} = 2.54$, $p < 0.05$, $d = 0.68$; 0 to 200 ms: $t_{(13)} = 2.04$, $p = 0.06$, $d = 0.54$) and the latency of peak FCz theta power (-100 to 300 ms: $t_{(13)} = -3.43$, $p < 0.01$, $d = 0.92$; 0 to 200 ms: $t_{(13)} = -5.25$, $p < 0.01$, $d = 1.4$) on the error trial predicted posterror slowing, with greater peak power and faster peak latencies predicting more reaction time slowing on the following trial. F5–FCz ICPS did not significantly predict posterror slowing (-100 to 300 ms: $t_{(13)} = 0.82$, $p > 0.10$, $d = 0.22$; 0 to 200 ms: $t_{(13)} = 1.13$, $p > 0.10$, $d = 0.30$), but F6–FCz ICPS did predict posterror slowing in the narrow time window (-100 to 300 ms: $t_{(13)} = 1.62$, $p > 0.10$, $d = 0.43$; 0 to 200 ms: $t_{(13)} = 2.86$, $p < 0.01$, $d = 0.77$). Additionally, we calculated congruency effects on single-trial analyses (supplemental Fig. S2, available at www.jneurosci.org as supplemental material). Overall, in all analyses shown in Figure 4 and supplemental Figure S2, available at www.jneurosci.org as supplemental material, the relationship between ICPS and FCz power is strong and distinct, whereas ICPS and FCz power metrics each moderately predicted posterror slowing.

Discussion

This investigation revealed that oscillatory synchrony in the theta band between mid-frontal and lateral frontal sites is increased

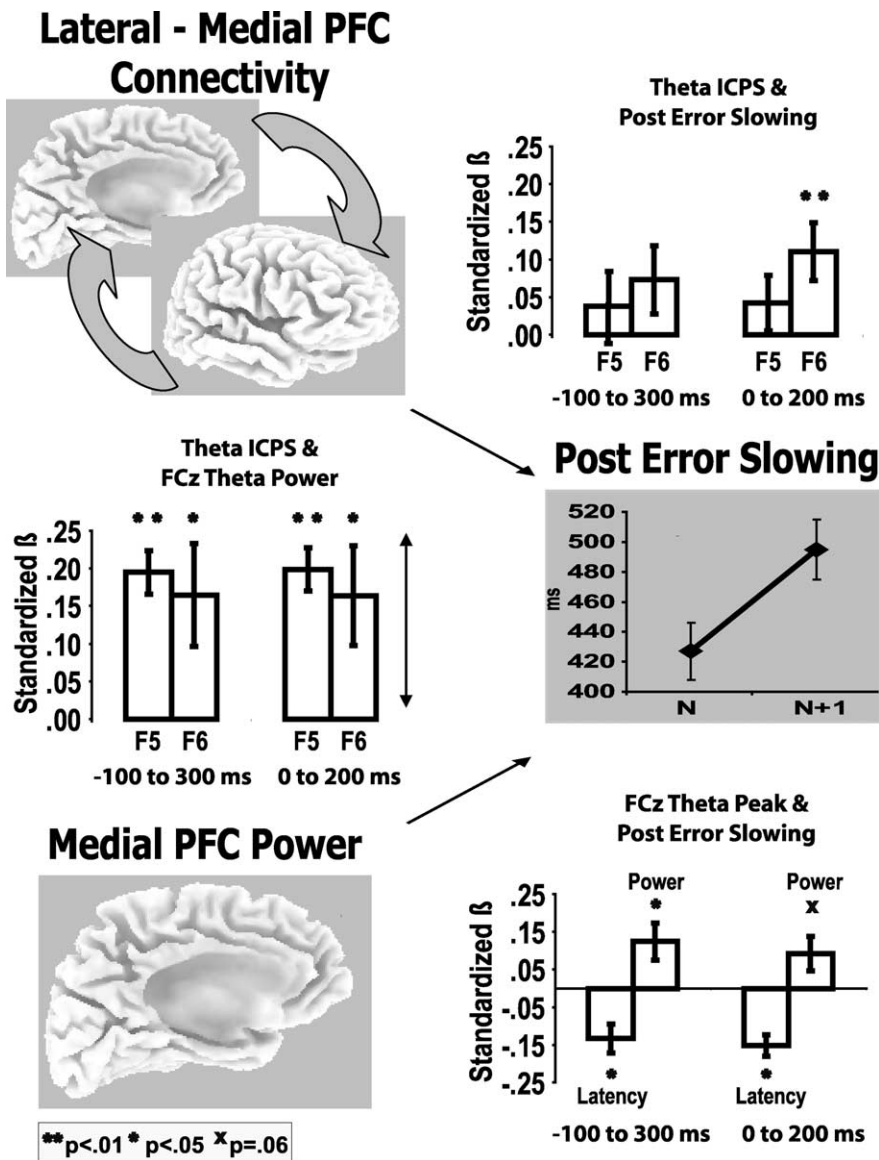


Figure 4. Single-trial analyses of the proposed cognitive control and action-monitoring network. Data from two different analytic windows are included: (–100 to 300 ms) and (0 to 200 ms). The degree of theta-band synchrony between IPFC and mPFC sites (ICPS) predicts the amount of FCz theta power increase. The degree of posterror slowing is predicted by both FCz theta power dynamics and theta ICPS.

immediately after response errors of commission. The degree of this oscillatory synchrony correlated with mid-frontal theta power increases, and both of these measures predicted the degree of posterror behavioral adjustment. The waning and waxing of mid-frontal activity during the prelude to and resolution of an error suggests that theta-band phase coherence and power dynamics reflect variability in the integrity of the action-monitoring system. Theta-band oscillatory synchrony between mPFC and IPFC may reflect a mechanism of communication between action-monitoring and cognitive control networks (Botvinick et al., 2001; Ridderinkhof et al., 2004a,b; Yeung et al., 2004a).

The roles of the action-monitoring and cognitive control networks

The conflict-control model of Botvinick et al. (2001) postulates that separate conflict-monitoring and cognitive control systems interact to optimize performance. When a large degree of re-

sponse conflict is encountered (such as during response errors), an alerting system in the ACC signals the need for enhanced cognitive control. This signal is transferred to IPFC among other regions, where it is used to adjust control over cognitive, motor, or emotion systems to optimize goal-directed performance (Kerns et al., 2004; Ridderinkhof et al., 2004b; Procyk et al., 2007). Other theories suggest that the ACC both detects conflict and acts to switch behavior (Rushworth et al., 2004, 2007; Kennerly et al., 2006). Behavioral adaptation may be informed by IPFC areas sensitive to task set and goal-oriented performance (Miller, 2000). Behavioral adaptation may be facilitated by altered mPFC activity, which could reallocate attention or increase the motor threshold to avoid further errors (Botvinick et al., 2001; Ullsperger and von Cramon, 2006; Eichele et al., 2008).

Multiple accounts of the action-monitoring system predict that the prelude to an error occurs when the integrity of the action-monitoring system diminishes over time, leading to high-conflict situations or errors (Botvinick et al., 2001; Allain et al., 2004; Weissman et al., 2006; Eichele et al., 2008). The resolution of an error may occur when the IPFC and mPFC systems interact to strategically adjust behavior, as shown by previous ERN and functional magnetic resonance imaging (fMRI) findings of increased ACC activity preceding larger posterror reaction time adjustments (Garavan et al., 2002; Kerns et al., 2004; Debener et al., 2005; Kerns, 2006; Hester et al., 2007). As noted above and described in previous studies, the ACC does not act alone: it works in concert with other cortical (IPFC) and subcortical structures to act during conflict or error signals to alter behavior. However, the mechanism of communication between these regions had not been specified in

previous studies. As discussed below, this investigation has provided novel evidence that oscillatory phase synchrony between medial and lateral PFC reflects a mechanism by which these critical cortical nodes in the action-monitoring and cognitive control networks may operate.

Oscillatory dynamics of the medial prefrontal action-monitoring system

The ACC has been shown to generate neural oscillations in the theta band (Wang et al., 2005; Tsujimoto et al., 2006), and these oscillations have been linked to several processes including memory, attention, feedback processing, and response errors (Onton et al., 2005; Wang et al., 2005; Cohen et al., 2007). Our findings add to a growing literature that suggests that neural oscillations in the theta range underlie conflict/error detection processes (Luu and Tucker, 2001; Luu et al., 2003, 2004; Trujillo and Allen, 2007; Cohen et al., 2008). The data from this investigation support the

idea that response errors are accompanied by enhanced medial frontal theta, and also suggests that the interaction between action-monitoring and cognitive control systems capitalize on these ongoing oscillatory theta dynamics.

The pattern of error-preceding and error-following mPFC oscillatory dynamics in this investigation suggests that demanding motor responses might always be characterized by phasic mid-frontal power and phase coherence increases, and that errors represent a special case of altered oscillatory dynamics. An ongoing background of oscillatory perturbation would fit with neurological models of the ERN, which have characterized the oscillatory perturbation and power increase specific to error trials (Luu et al., 2004; Trujillo and Allen, 2007). The proposal that errors capitalize on ongoing response-related oscillatory dynamics does not conflict with the major computational models of the ERN such as Hopfield energy (Yeung et al., 2004a) or temporal difference error (Holroyd and Coles, 2002). Rather, it suggests that either of these formulae (or any other yet-to-be-specified algorithm) could account for error-driven alteration of power values over an inherent response-related background of oscillatory perturbation. Indeed, theta oscillatory reorganization and power enhancement may be the neurobiological means by which these computations are performed.

The dissociation between power and phase coherence peak times suggests that phase coherence is a temporally constant response-related phenomenon, and that inherent increases in power and phase coherence are enhanced after errors. We were able to reveal this dissociation by using precue (instead of pre-response) baselines, because previous work has shown that oscillatory processes related to conflict monitoring may arise pre-response (Cohen et al., 2008). This dissociation also argues against an alternative view that theta oscillatory dynamics arise as a methodological consequence of filtering a nonoscillatory “burst” (Yeung et al., 2004b, 2007), because this view would predict that the time course of phase coherence and power would be the same. A temporally extended, frequency band-specific response supports the oscillatory hypothesis, because if the theta effect were a filter artifact, it would not last much longer than the window of the ERN [see also Trujillo and Allen (2007) for further arguments supporting the oscillatory hypothesis]. Although the ERN normally peaks at ~80 ms, the temporal dynamics of error-related activity occur across a wide window of time. Future EEG and fMRI investigations may endeavor to parse the temporal and spatial specificity of mPFC activity: both ERN and error positivity effects have been implicated in dorsal and rostral ACC within 300 ms of an error (Van Veen and Carter, 2002; Luu et al., 2003). It is unknown, however, if there are hemodynamic consequences of phase synchrony, because phase synchrony may occur in absence of overall changes in power. Thus, the executive network implicated by coherent oscillations between mPFC and lPFC regions may be uniquely assessed by EEG.

Oscillatory phase coherence between action-monitoring and cognitive control networks

Synchronous oscillations are thought to reflect a mechanism for entrained interregional activity. Rhythmic excitability may allow temporal windows of coordinated spike timing across spatially separate neural networks (Fries, 2005). Synchronous oscillations have been observed across multiple and disparate sites in the brain (König et al., 1995; Chawla et al., 2001; Nikouline et al., 2001; Freeman and Rogers, 2002), suggesting that information is transferred via wave packets (Rubino et al., 2006; Benucci et al., 2007). After an error, mPFC and lPFC sites showed synchronous

phase relations, suggesting that they had become transiently functionally linked. The lack of similar functional connectivity with posterior sites at a comparable distance from the mPFC site bolsters this argument of specific functional linking between mPFC and lPFC and not mere volume conduction of activity. In contrast to the interchannel phase synchrony, error-related power and phase coherence increases were demonstrated only in the mPFC (not lPFC). This dissociation between local error-related mPFC and lPFC activities suggests that the concurrent timing of oscillatory dynamics, and not power or response-locked phase coherence alone, underlies communication between these regions.

Adjusting future behavior

Given that mPFC–lPFC oscillatory coherence correlated with the degree of mPFC power increase, and both of these predicted the degree of posterror slowing, it is highly likely that these EEG dynamics reflect interrelated processes relevant to the detection and correction of errors. These effects were also larger on posterior trials that were incongruent (supplemental Fig. S2, available at www.jneurosci.org as supplemental material), similar to a recent study which revealed ACC–lPFC coupling in the theta band after incongruent trials in a Stroop task (Hanslmayr et al., 2008). Both the peak mPFC power and the latency of the peak predicted the degree of posterror slowing, suggesting that both the speed and magnitude of the error signal in the mPFC indicate the degree of conflict and need for subsequent behavioral adaptation. Future research may aim to parse the temporal and intensity dynamics of this error-related oscillatory readjustment (even occurring pre-response) as determinants of the severity of an error and latency of corrective adjustment.

Conclusions

We propose that inter-region oscillatory synchrony in the theta band may be one mechanism by which action-monitoring and cognitive control networks interact in the prefrontal cortex. This long-range oscillatory synchrony may capitalize on an inherent background of medial frontal theta-band oscillatory perturbation and power increase during manual responses. Errors may induce altered oscillatory and power dynamics in this system, which in turn support enhanced computation and interregional communication. The findings of this investigation suggest that the dynamic oscillatory interplay between medial and lateral frontal regions underlies our ability to detect errors and adjust behavior accordingly.

References

- Allain S, Carbone L, Falkenstein M, Burle B, Vidal F (2004) The modulation of the Ne-like wave on correct responses foreshadows errors. *Neurosci Lett* 372:161–166.
- Benucci A, Frazor RA, Carandini M (2007) Standing waves and traveling waves distinguish two circuits in visual cortex. *Neuron* 55:103–117.
- Botvinick MM, Braver TS, Barch DM, Carter CS, Cohen JD (2001) Conflict monitoring and cognitive control. *Psychol Rev* 108:624–652.
- Cavanagh JF, Allen JJB (2008) Multiple aspects of the stress response under social evaluative threat: an electrophysiological investigation. *Psychoneuroendocrinology* 33:41–53.
- Chawla D, Friston KJ, Lumer ED (2001) Zero-lag synchronous dynamics in triplets of interconnected cortical areas. *Neural Netw* 14:727–735.
- Cohen MX, Elger CE, Ranganath C (2007) Reward expectation modulates feedback-related negativity and EEG spectra. *Neuroimage* 35:968–978.
- Cohen MX, Ridderinkhof R, Haupt S, Elger CE, Fell J (2008) Medial frontal cortex and response conflict: evidence from human intracranial EEG and medial frontal cortex lesion. *Brain Res* 1238:127–142.
- Debener S, Ullsperger M, Siegel M, Fiehler K, von Cramon DY, Engel AK

- (2005) Trial-by-trial coupling of concurrent electroencephalogram and functional magnetic resonance imaging identifies the dynamics of performance monitoring. *J Neurosci* 25:11730–11737.
- Eichele T, Debener S, Calhoun VD, Specht K, Engel AK, Hugdahl K, von Cramon DY, Ullsperger M (2008) Prediction of human errors by maladaptive changes in event-related brain networks. *Proc Natl Acad Sci U S A* 105:6173–6178.
- Engel AK, Singer W (2001) Temporal binding and the neural correlates of sensory awareness. *Trends Cogn Sci* 5:16–25.
- Eriksen BA, Eriksen CW (1974) Effects of noise letters upon the identification of target letters in a non-search task. *Percept Psychophys* 16:143–149.
- Eriksen CW, Schultz DW (1979) Information processing in visual search: a continuous flow conception and experimental results. *Percept Psychophys* 24:249–263.
- Freeman WJ, Rogers LJ (2002) Fine temporal resolution of analytic phase reveals episodic synchronization by state transitions in gamma EEGs. *J Neurophysiol* 87:937–945.
- Fries P (2005) A mechanism for cognitive dynamics: neuronal communication through neuronal coherence. *Trends Cogn Sci* 9:474–480.
- Garavan H, Ross TJ, Murphy K, Roche RA, Stein EA (2002) Dissociable executive functions in the dynamic control of behavior: inhibition, error detection, and correction. *Neuroimage* 17:1820–1829.
- Gehring WJ, Fencsik DE (2001) Functions of the medial frontal cortex in the processing of conflict and errors. *J Neurosci* 21:9430–9437.
- Hanslmayr S, Pastötter B, Bäuml KH, Gruber S, Wimber M, Klimesch W (2008) The electrophysiological dynamics of interference during the Stroop task. *J Cogn Neurosci* 20:215–225.
- Hester R, Barre N, Mattingley JB, Foxe JJ, Garavan H (2007) Avoiding another mistake: error and posterror neural activity associated with adaptive posterror behavior change. *Cogn Affect Behav Neurosci* 7:317–326.
- Holroyd CB, Coles MG (2002) The neural basis of human error processing: reinforcement learning, dopamine, and the error-related negativity. *Psychol Rev* 109:679–709.
- Kayser J, Tenke CE (2006) Principal components analysis of Laplacian waveforms as a generic method for identifying ERP generator patterns: II. Adequacy of low-density estimates. *Clin Neurophysiol* 117:369–380.
- Kennerley SW, Walton ME, Behrens TE, Buckley MJ, Rushworth MF (2006) Optimal decision making and the anterior cingulate cortex. *Nat Neurosci* 9:940–947.
- Kerns JG (2006) Anterior cingulate and prefrontal cortex activity in an fMRI study of trial-to-trial adjustments on the Simon task. *Neuroimage* 33:399–405.
- Kerns JG, Cohen JD, MacDonald AW 3rd, Cho RY, Stenger VA, Carter CS (2004) Anterior cingulate conflict monitoring and adjustments in control. *Science* 303:1023–1026.
- König P, Engel AK, Roelfsema PR, Singer W (1995) How precise is neuronal synchronization? *Neural Comput* 7:469–485.
- Luu P, Tucker DM (2001) Regulating action: alternating activation of midline frontal and motor cortical networks. *Clin Neurophysiol* 112:1295–1306.
- Luu P, Tucker DM, Derryberry D, Reed M, Poulsen C (2003) Electrophysiological responses to errors and feedback in the process of action regulation. *Psychol Sci* 14:47–53.
- Luu P, Tucker DM, Makeig S (2004) Frontal midline theta and the error-related negativity: neurophysiological mechanisms of action regulation. *Clin Neurophysiol* 115:1821–1835.
- Miller EK (2000) The prefrontal cortex and cognitive control. *Nat Rev Neurosci* 1:59–65.
- Nikouline VV, Linkenkaer-Hansen K, Huttunen J, Ilmoniemi RJ (2001) Interhemispheric phase synchrony and amplitude correlation of spontaneous beta oscillations in human subjects: a magnetoencephalographic study. *Neuroreport* 12:2487–2491.
- Onton J, Delorme A, Makeig S (2005) Frontal midline EEG dynamics during working memory. *Neuroimage* 27:341–356.
- Procyk E, Amiez C, Quilodran R, Joseph JP (2007) Modulations of prefrontal activity related to cognitive control and performance monitoring. In: *Sensorimotor foundations of higher cognition attention and performance: attention and performance XXII* (Haggard P, Rossetti Y, Kawato M, eds), pp 27–46. New York: Oxford UP.
- Ridderinkhof KR, Nieuwenhuis S, Bashore TR (2003) Errors are foreshadowed in brain potentials associated with action monitoring in cingulate cortex in humans. *Neurosci Lett* 348:1–4.
- Ridderinkhof KR, van den Wildenberg WP, Segalowitz SJ, Carter CS (2004a) Neurocognitive mechanisms of cognitive control: the role of prefrontal cortex in action selection, response inhibition, performance monitoring, and reward-based learning. *Brain Cogn* 56:129–140.
- Ridderinkhof KR, Ullsperger M, Crone EA, Nieuwenhuis S (2004b) The role of the medial frontal cortex in cognitive control. *Science* 306:443–447.
- Rubino D, Robbins KA, Hatsopoulos NG (2006) Propagating waves mediate information transfer in the motor cortex. *Nat Neurosci* 9:1549–1557.
- Rushworth MF, Walton ME, Kennerley SW, Bannerman DM (2004) Action sets and decisions in the medial frontal cortex. *Trends Cogn Sci* 8:410–417.
- Rushworth MF, Buckley MJ, Behrens TE, Walton ME, Bannerman DM (2007) Functional organization of the medial frontal cortex. *Curr Opin Neurobiol* 17:220–227.
- Trujillo LT, Allen JJ (2007) Theta EEG dynamics of the error-related negativity. *Clin Neurophysiol* 118:645–668.
- Tsujimoto T, Shimazu H, Isomura Y (2006) Direct recording of theta oscillations in primate prefrontal and anterior cingulate cortices. *J Neurophysiol* 95:2987–3000.
- Ullsperger M, von Cramon DY (2006) How does error correction differ from error signaling? An event-related potential study. *Brain Res* 1105:102–109.
- Van Veen V, Carter CS (2002) The timing of action-monitoring processes in the anterior cingulate cortex. *J Cogn Neurosci* 14:593–602.
- Wang C, Ulbert I, Schomer DL, Marinkovic K, Halgren E (2005) Responses of human anterior cingulate cortex microdomains to error detection, conflict monitoring, stimulus-response mapping, familiarity, and orienting. *J Neurosci* 25:604–613.
- Weissman DH, Roberts KC, Visscher KM, Woldorff MG (2006) The neural bases of momentary lapses in attention. *Nat Neurosci* 9:971–978.
- Yeung N, Botvinick MM, Cohen JD (2004a) The neural basis of error detection: conflict monitoring and the error-related negativity. *Psychol Rev* 111:931–959.
- Yeung N, Bogacz R, Holroyd CB, Cohen JD (2004b) Detection of synchronized oscillations in the electroencephalogram: an evaluation of methods. *Psychophysiology* 41:822–832.
- Yeung N, Bogacz R, Holroyd CB, Nieuwenhuis S, Cohen JD (2007) Theta phase resetting and the error-related negativity. *Psychophysiology* 44:39–49.